I-EDU GROUP

Article

Title: Modern approaches to water balance models and ecosystem stability assessment in the Aydar-Arnasay lake system: analysis and prospects.

Aybek Arifjanov [1], Lukmon Samiev [1], Jalilov Sirojiddin [1,2,3]*, Arken Tursun [2,5], Jalilova Khumora [1], Reimbayev Mardon [1]

[1] Tashkent Institute of Irrigation and Agricultural Mechanization Engineers, National Research University, Tashkent 100000, Uzbekistan.
[2] State Key Laboratory of Ecological Safety and Sustainable Development in Arid Lands, Xinjiang Institute of Ecology and Geography, Chinese Academy of Science, Urumqi 830011, China.
[3] Xinjiang Key Laboratory of RS GIS Application, Urumqi 830011, China.
[4] University of Chinese Academy of Sciences, Beijing 100049, China.
[5] Sino-Belgian Joint Laboratory for Geo-Information, Urumqi 830011, China.
* Correspondence: Jalilov Sirojiddin, Email: s.jalilov@tiiame.uz

Abstract: Efficient hydraulic design of drip irrigation systems requires pipe sizing that accounts for the spatial distribution of irrigation demand and the sequence of system operation. When pump capacity limits the area irrigated simultaneously, different combinations of active subplots can produce different hydraulic conditions despite maintaining the same total discharge. This study develops a method that integrates spatial subplot grouping into operating shifts with hydraulic network analysis to support pipe diameter selection. The method combines equal-area field subdivision, max–min pairing based on centroid distances, pump discharge constraints, and hydraulic calculations for each operating shift. An irregular field of approximately 19.02 ha was divided into 12 subplots and organized into six paired shifts. Each planned shift covered approximately 3.17 ha at a discharge of 111.24 m^3 h^{-1}, with a scheduled irrigation sequence lasting 18.81 h. Centroid distances between paired subplots ranged from 287.20 to 349.24 m. Preliminary hydraulic calculations covering 11 connected subplots showed that the five complete paired shifts required pumping heads of 22.71-25.00 m at approximately equal inlet discharge. The maximum mainline velocity was 0.98 m s^{-1}, below the adopted limit of 2.2 m s^{-1}. These results demonstrate that equal discharge does not eliminate differences in hydraulic loading and that pipe sizing must consider the governing operating shift. The proposed approach can support preliminary design and operational assessment of drip irrigation networks on irregular fields where pump capacity requires rotational irrigation, providing a basis for comparing subplot groupings and evaluating commercial pipe diameters.

Keyword: drip irrigation; spatial subplot pairing; rotational irrigation; max–min optimization; pipe sizing; hydraulic network analysis

Quoting: Aybek Arifjanov, Lukmon Samiev, Jalilov Sirojiddin, Arken Tursun, Jalilova Khumora, Reimbayev Mardon. Optimizing Pipe Diameters in Drip Irrigation Systems through Spatial Grouping of Subplots into Irrigation Shifts. **2026**, 4, 2, 1. https://doi.org/10.35938/jhee-2026-1-00006

Received: 23.10.2026
Corrected: 25.10.2026
Accepted: 29.10.2026
Published: 30.10.2026

Copyright:

OPEN ACCESS

Check for updates

CC BY

Introduction

Limited water availability has increased the need to improve irrigation performance and the management of agricultural water supplies [1] . Drip irrigation enables controlled water application near the crop root zone and can improve water productivity under appropriate design and management conditions [2]. Its performance depends on the hydraulic configuration of the distribution network and the operating conditions of the emitters [3]. Pressure differences along the network can affect emitter discharge and irrigation uniformity, particularly when non-pressure-compensating emitters are used [4].

Pipe diameter is a principal design variable because it influences flow velocity, friction losses, and the pressure available at downstream outlets [5]. Increasing pipe diameter generally reduces friction losses but increases pipe procurement costs. Conversely, smaller diameters can increase the pumping head required to maintain adequate pressure at the emitters. Diameter selection therefore

requires an assessment of both hydraulic feasibility and economic performance [6]. When the available pump discharge cannot supply the entire field simultaneously, irrigation subplots can be organized into groups that operate in successive shifts [7]. The composition of each shift determines which outlets are active and, consequently, the discharge passing through individual pipe sections. Different combinations of simultaneously irrigated subplots can produce different flow distributions, even when the total operating discharge remains unchanged [8]. Pipe sizing should therefore account for the hydraulic conditions associated with all scheduled shifts.

The spatial arrangement of active subplots also influences the routes through which water is conveyed from the pump to the irrigation units [9]. Grouping adjacent subplots may concentrate demand within a shared branch, whereas operating spatially separated subplots may distribute demand across different branches. The resulting hydraulic effect depends on the network topology, pump location, elevation differences, and the lengths of the supply paths [10]. Consequently, a larger distance between paired subplots does not, by itself, establish that smaller pipe diameters or lower head losses will be achieved.

Previous studies have applied mathematical programming and heuristic optimization methods to the design of pressurized irrigation networks [11]. Genetic algorithms have been used to optimize pipe diameters and pipeline layouts under hydraulic constraints [genetic algorithm; simultaneous pipeline layout and diameter optimization; drip irrigation network]. Particle swarm optimization and hybrid methods have also been investigated for selecting network parameters and reducing system costs [12]. Studies incorporating pumping costs further demonstrate the importance of evaluating the relationship between pipe investment and operating energy requirements [13].

These considerations motivate an assessment of subplot grouping as a design decision linked to pipe sizing. In the approach examined here, subplots are paired using a max–min criterion that maximizes the shortest distance among all selected pairs. This formulation is related to the bottleneck matching problem, in which the quality of a complete matching is determined by its least favorable pair [14]. The criterion evaluates the complete pairing arrangement rather than selecting the most distant pair at each successive step. Hydraulic calculations are then required to determine how the selected arrangement affects discharge, velocity, and pressure throughout the network. Several software tools have been developed to support the hydraulic design and evaluation of microirrigation systems. MIRRIG combines design, simulation, and multicriteria analysis to compare alternatives using technical, economic, and environmental criteria [15] . PRESUD supports the economic design of rectangular microirrigation subunits through iterative calculations of lateral and manifold pipelines [16]. Its extension, PRESUD-IR, considers irregular plot shapes and topographic conditions when evaluating water application costs and emission uniformity [17]. Other programs provide complementary approaches to component sizing and hydraulic assessment. IrriLab uses explicit analytical relationships to determine design variables for rectangular microirrigation units on uniform slopes, including inlet pressure, discharge, and manifold diameter [18]. DIMSUB provides an Excel-based environment for evaluating subunit configurations in terms of water distribution, pressure requirements, and material costs [19]. DOMIS supports microirrigation system design and cost estimation [20]. HydroCalc has also been applied to evaluate and select drip irrigation system designs.

Hydraulic simulation and spatial design have increasingly been incorporated into computational workflows. EPANET has been used to model an operating drip irrigation network and assess its hydraulic performance against field observations [21]. QDrip integrates QGIS-based spatial layout, EPANET hydraulic simulation, and genetic algorithm optimization to select pipe configurations and subunit inlet pressure according to an annual cost objective [22]. A web-based submain design application additionally enables designers to examine outlet pressure heads and pressure variation under uniform and non-uniform slope conditions [23].

Building on these computational approaches, this study aims to develop and evaluate a method for selecting pipe diameters by integrating the spatial grouping of irrigation subplots into operating shifts with hydraulic network analysis. The method uses max–min pairing subject to pump discharge constraints, followed by shift-specific hydraulic calculations and the selection of commercially available pipe diameters that satisfy velocity and pressure requirements. The proposed approach is compared with adjacent-subplot grouping under the same field geometry, irrigation requirements, pump capacity, and hydraulic limits. Performance is assessed using pipe-section discharges, selected

diameters, flow velocities, required pumping head, residual pressure, and pipe procurement costs. This comparison determines whether spatial pairing can reduce pipe procurement costs while maintaining the required hydraulic performance.

Materials and Methods

2.1.0. Spatial Pairing of Subplots Using the Max–Min Principle

Simply selecting the two most distant plots is insufficient, as this may leave the remaining plots close to one another. Therefore, the developed algorithm evaluates the pairings collectively rather than individually. The principal criterion is to maximize the minimum distance among all selected pairs, following the max–min principle.

At the initial calculation stage, the geometric centroid of each plot is determined. For a rectangular plot, the centroid coordinates are calculated as follows:

$$x_i = \frac{x_{i,\min} + x_{i,\max}}{2}, \qquad y_i = \frac{y_{i,\min} + y_{i,\max}}{2} \tag{1}$$

where x_i and y_i are the horizontal and vertical coordinates of the centroid of plot i (m); $x_{i,\min}$ and $x_{i,\max}$ are the minimum and maximum horizontal boundary coordinates, respectively; and $y_{i,\min}$ and $y_{i,\max}$ are the minimum and maximum vertical boundary coordinates, respectively. For irregularly shaped plots, the software determines the centroid using the polygon geometry. When geographic coordinates are provided, they are converted to a suitable projected coordinate reference system with metric units before distances are calculated.

Once the centroids have been determined, the distances between all possible pairs of plots are calculated using the Euclidean distance formula based on the Pythagorean theorem:

$$d_{ij} = \sqrt{(x_i - x_j)^2 + (y_i - y_j)^2} \tag{2}$$

where d_{ij} is the straight-line distance between the centroids of plots i and j (m). The coordinate differences represent the horizontal and vertical separation between the two centroids. This distance is used as a criterion for pairing plots; it does not represent the actual pipe length or the shortest distance between plot boundaries.

The next pairing constraint concerns the pump's operating flow rate. The combined flow requirement of two plots irrigated simultaneously must satisfy the following condition:

$$Q_i + Q_j \leq Q_{\text{pump}} \tag{3}$$

where Q_i and Q_j are the design flow rates of the respective plots ($m^3\ h^{-1}$), and Q_{pump} is the available pump discharge ($m^3\ h^{-1}$). This constraint prevents plots whose combined flow requirement exceeds the pump capacity from being grouped within a single irrigation shift. All plots must be paired, and each plot must belong to exactly one irrigation shift.

For each feasible pairing configuration, the minimum distance among all selected pairs is determined as follows:

$$D(P) = \min_{(i,j)\in P} d_{ij} \tag{4}$$

where P represents a feasible configuration that partitions all plots into pairs, and $D(P)$ is the minimum centroid distance among the selected pairs in that configuration.

"'latex The minimum pair distance in this configuration, m. For example, if the three pair distances in a configuration are 223.6, 223.6, and 100.0 m, its evaluation score is 100.0 m.

The main equation of the plot-pairing model is expressed as follows:

$$P^* = \arg\max_{P\in\mathcal{P}} \left[\min_{(i,j)\in P} \sqrt{(x_i - x_j)^2 + (y_i - y_j)^2} \right] \tag{5}$$

Here, D — The maximum achievable minimum distance under the given plot layout and flow-rate constraints. Thus, Equation (4.5) determines which pairs are selected, while Equation (4.6) represents the distance-based outcome of the selected configuration.

In the software implementation, plots are represented as graph nodes, while feasible pairings are represented as edges connecting them. For a specified distance threshold, only pairs whose separation is at least equal to that threshold and that satisfy the flow-rate constraint are considered (Figure 1).

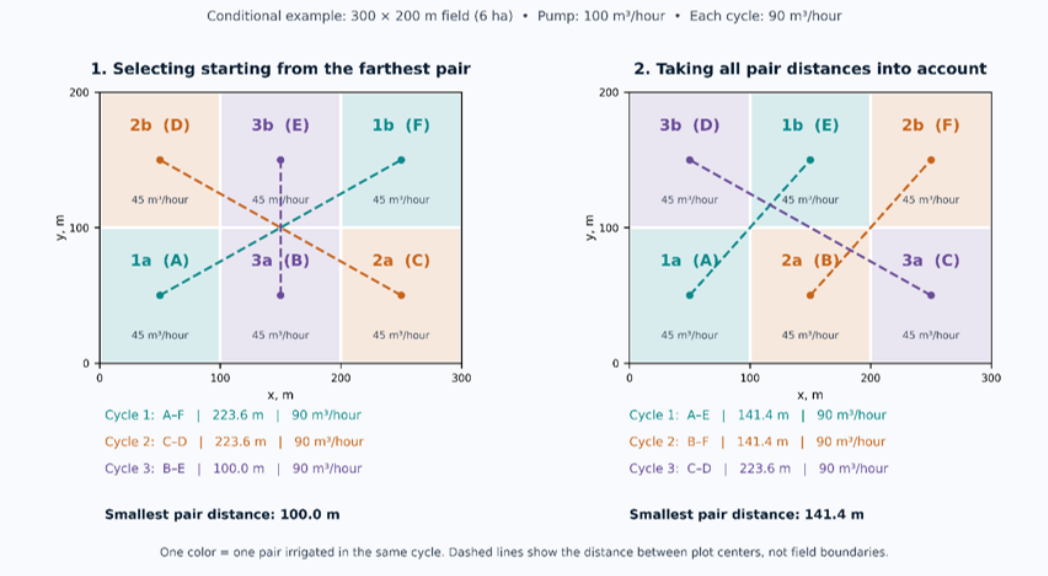

Figure 1. Pairing plots with their farthest counterpart

The algorithm then checks whether a perfect matching covering all plots can be formed using these edges. The distance threshold is refined to identify the largest value for which a perfect matching remains feasible. This optimization is performed on the previously generated plots; it does not encompass all possible field subdivision configurations.

Results

Field subdivision and spatial grouping of irrigation subplots

The irregularly shaped field was divided into 12 irrigation subplots, each with a reported area of approximately 1.585 ha, giving a total irrigated area of approximately 19.02 ha (Figure 1). Equal-area subdivision was maintained despite differences in subplot shape along the field boundary. Consequently, the allocation of irrigation area was consistent across subplots, while their geometry reflected the available field configuration.

The subplots were organized into six irrigation shifts, with two subplots operating simultaneously in each shift. Each pair was identified by a common number and the suffixes “a” and “b”: 1a–1b, 2a–2b, 3a–3b, 4a–4b, 5a–5b, and 6a–6b. The simultaneously irrigated area was therefore approximately 3.17 ha per shift, equivalent to 16.7% of the total field area. This arrangement maintained an equal active area across all six shifts.

Figure 2. Field subdivision into 12 equal-area irrigation subplots and their allocation to six operating shifts

The paired subplots were distributed across different parts of the field. For example, subplot 1a occupied the lower-left boundary, whereas its partner, 1b, was located in the upper-central part. Similarly, subplot 6a was positioned in the lower-right section, while 6b was situated toward the upper-left section. These arrangements illustrate how each shift combined spatially separated irrigation areas (Figure 2).

The pump, marked "N," supplied a mainline extending through the central part of the field. Distribution pipes connected the mainline to the individual subplots, within which the drip laterals were arranged. This configuration established the correspondence between subplot location, irrigation shift, and water delivery route, providing the spatial basis for the subsequent calculation of shift-specific pipe discharges and hydraulic requirements.

Irrigation schedule and subplot discharge requirements

The resulting irrigation schedule comprised six successive shifts, each supplying two paired subplots simultaneously (Figure 2). Each subplot had an area of 1.5852 ha and a calculated discharge of 55.6197 $m^3\ h^{-1}$. Accordingly, the simultaneously irrigated area was 3.1704 ha per shift, with a combined discharge of approximately 111.239 $m^3\ h^{-1}$. The identical discharge requirements across all six shifts established a consistent demand at the system inlet.

The distances between paired subplot centroids ranged from 287.204 to 349.242 m, with a mean of 317.446 m. The largest separation occurred in Shift 1, between subplots 1a and 1b, whereas the smallest occurred in Shift 5, between subplots 5a and 5b. The corresponding distances for Shifts 2, 3, 4, and 6 were 323.981, 319.947, 314.222, and 310.082 m, respectively. Thus, the minimum pair distance achieved by the selected arrangement was 287.204 m. These distances characterize the spatial separation of simultaneously irrigated subplots and should be distinguished from the actual water conveyance path lengths.

Irrigation schedule

Cycle	Plots	Flow, m³/hour	Smallest distance, m	Time, hours
1	1a + 1b	111.239	349.242	3.135
2	2a + 2b	111.239	323.981	3.135
3	3a + 3b	111.239	319.947	3.135
4	4a + 4b	111.239	314.222	3.135
5	5a + 5b	111.239	287.204	3.135
6	6a + 6b	111.239	310.082	3.135

Plots

Plot	Cycle	Area, ha	Flow, m³/hour
1a	1	1.5852	55.6197
1b	1	1.5852	55.6197
2a	2	1.5852	55.6197
2b	2	1.5852	55.6197
3a	3	1.5852	55.6197
3b	3	1.5852	55.6197
4a	4	1.5852	55.6197
4b	4	1.5852	55.6197
5a	5	1.5852	55.6197

Figure 3. Irrigation schedule and subplot characteristics, showing the paired subplots, combined discharge, centroid separation, and operating duration for each shift.

The scheduled irrigation duration was 3.135 h for every shift. Completing all six shifts sequentially therefore required 18.81 h, equivalent to approximately 18 h and 49 min. Equal subplot areas and discharge requirements produced equal scheduled irrigation durations, while the locations of the active subplots changed between shifts. Consequently, the hydraulic assessment must account for different flow distributions within the network under the same total inlet discharge.

Hydraulic performance of hydrants, drip laterals, and distribution pipes

The hydraulic calculation tables covered 11 subplots, each with a listed design discharge of approximately 55.6 $m^3 h^1$ (Figure 3). The combined head loss in the mainline and connector pipes ranged from 0.45 to 2.28 m. The lowest value occurred along the supply route to subplot 2a, whereas the highest occurred along the route to subplot 4b. Head losses within the distribution pipes ranged from 0.06 m in subplot 5b to 1.93 m in subplot 6b.

The calculated pressure head at the hydrants varied between 12.7 and 14.5 m, while the required pressure head at the drip-lateral inlet ranged from 10.39 to 12.20 m. The reported excess head ranged from 0.0 to 2.6 m. Subplot 4b represented the critical supply route, combining the highest mainline-plus-connector loss of 2.28 m with the lowest hydrant pressure head of 12.7 m. Its excess head was displayed as 0.0 m, indicating negligible remaining pressure margin at the reported precision. By comparison, subplot 2a had the largest excess head, at 2.6 m.

Hydrants

Plot	Hydrant	Cycle	Flow, m³/hour	Along main, m	Connector, m	Main + connector, m	Distributor, m	Tape inlet, m	Head at hydrant, m	Excess head, m
1b	G1	1	55.6	246	30	1.12	1.92	10.51	13.9	1.4
2a	G2	2	55.6	90	0	0.45	1.54	10.39	14.5	2.6
2b	G2	2	55.6	320	30	1.55	1.91	10.52	13.4	1.0
3a	G3	3	55.6	157	0	0.79	1.37	10.50	14.2	2.3
3b	G3	3	55.6	395	30	1.91	1.90	10.53	13.1	0.7
4a	G4	4	55.6	231	0	1.17	1.19	10.69	13.8	2.0
4b	G4	4	55.6	471	30	2.28	1.89	10.83	12.7	0.0
5a	G5	5	55.6	314	0	0.68	0.98	11.04	14.3	2.3
5b	G5	5	55.6	67	29	1.10	0.06	11.36	13.9	2.5
6a	G6	6	55.6	410	0	1.20	0.75	12.20	13.8	0.8
6b	G6	6	55.6	172	30	1.65	1.93	10.50	13.4	0.9

Tapes and distributor pipes

Plot	Number of tapes	Total length, m	Longest tape, m	Tape loss, m	Distributor length, m	Distributor velocity, m/s
1b	141	10440	74.4	0.68	212	1.63
2a	161	10436	67.5	0.52	242	1.43
2b	140	10436	74.8	0.69	210	1.63
3a	149	10498	73.9	0.67	223	1.42
3b	139	10431	75.3	0.70	209	1.63
4a	135	10509	82.7	0.92	201	1.40
4b	139	10434	88.2	1.10	208	1.63
5a	119	10493	95.5	1.38	177	1.37
5b	142	10432	105.0	1.82	7	1.63
6a	101	10529	124.3	2.93	150	1.32
6b	142	10440	74.0	0.67	213	1.63

Losses are calculated with the Hazen-Williams formula; the flow along the distributor pipe and tapes is reduced by evenly distributed outlets (Christiansen coefficient); tape inlet head = emitter head + 0.75·tape loss; local losses are given as a percentage; the elevation difference is a single value. "Excess head" is how much the pump head exceeds what is needed for that hydrant (a pressure regulator may be required). This is a preliminary calculation, not a final design.

Drawing PNG | Table CSV | Plots GeoJSON | Plots CSV

Figure 4. Calculated hydraulic characteristics of hydrants, drip laterals, and distribution pipes, including supply-path losses, pressure requirements, excess head, lateral dimensions, and distribution-pipe velocities.

The number of drip laterals varied from 101 to 161 per subplot, although their total installed length remained within a relatively narrow range of 10,431–10,529 m. The longest individual lateral in each subplot ranged from 67.5 to 124.3 m. Subplot 6a contained the longest lateral, at 124.3 m, and exhibited the highest calculated lateral head loss of 2.93 m. Subplot 2a had the shortest maximum lateral length, at 67.5 m, and the lowest lateral head loss of 0.52 m. Thus, similar total lateral lengths were associated with different individual lateral lengths and hydraulic losses.

Distribution-pipe lengths ranged from 7 to 242 m, and the calculated velocities ranged from 1.32 to 1.63 m s^{-1}. The results identified different limiting components across the network: subplot 6a had the greatest lateral head loss, whereas subplot 4b had the smallest overall pressure margin. These findings highlight the importance of evaluating the complete supply route when assessing each subplot.

Because subplot 1a was absent from the hydraulic tables, the results represent a preliminary assessment of the connected subplots. Verification of the complete 12-subplot configuration requires inclusion of the missing subplot and recalculation of the affected operating shift.

The calculated pumping head varied from 22.71 to 25.00 m across the six reported irrigation shifts (Figure 4). Shift 4 represented the governing operating condition, requiring a head of 25.00 m at a discharge of approximately 111.2 m^3 h^{-1}. Subplot 4b was identified as the critical subplot in this shift, which also exhibited the highest mainline head loss of 1.50 m. The maximum calculated pumping head corresponded to approximately 2.45 bar.

Hydraulic calculation

Required pump head: **25.0 m** (≈ 2.45 bar), flow 111.2 m³/hour.

Maximum velocity in the main line is 0.98 m/s (limit 2.2 m/s).

There is a hydrant outside the plot.

Hydrant not placed: 1a

By cycle

Cycle	Hydrants opened	Flow, m³/hour	Critical plot	Main line loss, m	Required head, m
1	G1 (1b)	55.6	1b	0.34	23.56
2	G2 (2a, 2b)	111.2	2b	0.77	23.99
3	G3 (3a, 3b)	111.2	3b	1.12	24.34
4	G4 (4a, 4b)	111.2	4b	1.50	25.00
5	G5 (5b, 5a)	111.2	5a	0.68	22.71
6	G6 (6b, 6a)	111.2	6a	1.20	24.15

Figure 5. Preliminary pumping head requirements and mainline hydraulic performance by irrigation shift, including active hydrants, discharge, critical subplot, and mainline head loss.

The lowest pumping head requirement occurred in Shift 5, at 22.71 m, with a mainline head loss of 0.68 m. The difference between the highest and lowest pumping head requirements was therefore 2.29 m. Shifts 2, 3, and 6 required pumping heads of 23.99, 24.34, and 24.15 m, respectively. Although these five complete paired shifts had the same total discharge, their mainline head losses ranged from 0.68 to 1.50 m, demonstrating that the spatial distribution of active subplots influenced network loading.

The maximum calculated mainline velocity was 0.98 m s^{-1}, which remained 1.22 m s^{-1} below the specified limit of 2.2 m s^{-1}. Thus, the modeled mainline satisfied the adopted maximum-velocity criterion for the reported operating configurations.

Shift 1 differed from the other shifts because only subplot 1b was included in the hydraulic calculation. Consequently, its discharge was 55.6 m^3 h^{-1}, with a mainline head loss of 0.34 m and a required pumping head of 23.56 m. The system interface also identified a hydrant located outside the field boundary and a missing hydrant connection for subplot 1a. Therefore, the reported operating requirement of 25.00 m at 111.2 m^3 h^{-1} should be considered preliminary. Final verification requires correction of the hydrant locations, connection of subplot 1a, and recalculation of all irrigation shifts.

Validation of results

To verify the internal consistency of the hydraulic calculation, the tabulated results were independently recalculated and compared with the values produced by the model. Four checks were performed across the 11 irrigated plots and 6 irrigation cycles. According to the model's assumptions, the head at the tape inlet equals the emitter operating head (10 m) plus 0.75 of the head loss along the tape. Recalculating this value from the tabulated tape losses gave results that lie on the 1:1 line

for all plots (Figure 4). The maximum absolute difference was 0.005 m, which is within the rounding precision of the tables.

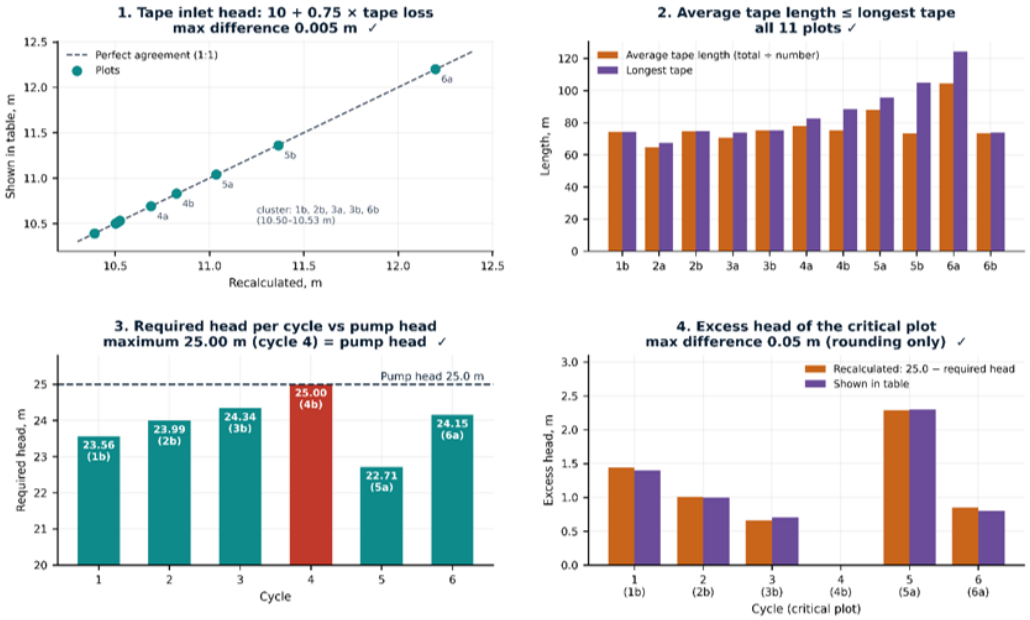

Figure 6. Validation of the hydraulic calculation

For every plot, the mean tape length (total tape length divided by the number of tapes) was smaller than the longest tape (panel 2). This is a necessary condition for geometric consistency, and it was satisfied in all 11 cases. The largest spread between the mean and the longest tape occurred in plots 5b and 6a.

The required head was computed for each cycle (panel 3). The highest value, 25.00 m, occurred in cycle 4 (plot 4b), which coincides with the pump head specified for the system. This confirms that the pump head is governed by the most demanding cycle and that no cycle exceeds the available head.

For the critical plot of each cycle, the excess head was recalculated as the difference between the pump head (25.0 m) and the required head (panel 4). The recalculated and tabulated values differed by no more than 0.05 m, attributable to rounding. Cycle 4 had zero excess head, whereas cycle 5 had the largest margin (2.3 m), so pressure regulation may be needed in the cycles with more excess head.

This validation checks the arithmetic and logical consistency of the results. It is not an experimental validation against field measurements. In addition, the irrigation time (3.135 h) could not be reproduced from the tabulated data alone. The distributor length for plot 5b (7 m) is much shorter than in the other plots (150–240 m) and should be checked against the hydrant placement, and no hydrant was placed for plot 1a.

Discussion

The hydraulic results demonstrate that equal discharge at the system inlet does not ensure equal pressure requirements across irrigation shifts. At approximately 111.2 m^3 h^{-1}, the five complete paired shifts required pumping heads ranging from 22.71 to 25.00 m. This difference indicates that the locations of simultaneously operating subplots affect flow distribution throughout the network. A related finding was reported in [24], where irrigation scheduling was optimized using individual sprinklers rather than entire branches as the minimum operating unit. Their approach reduced irrigation costs by approximately 18% compared with optimized branch scheduling. Although their study focused on sprinkler irrigation, it supports the broader interpretation that the spatial composition of operating groups can influence hydraulic and economic performance.

The importance of spatial configuration is also supported, who optimized drip irrigation network connectivity using a graph-based hydraulic model and a genetic algorithm. In their illustrative problem involving 49 fruit trees, the optimized topology reduced the coefficient of variation of emitter

discharge by 70%. Their objective directly addressed discharge uniformity, whereas the present method maximizes the minimum centroid distance between paired subplots. This distinction matters because improved spatial separation does not necessarily produce improved hydraulic performance. The pairing criterion provides a reproducible arrangement, but its consequences must be assessed using the actual network connections, pipe lengths, and pressure requirements.

The relationship between spatial decisions and pipe sizing was examined more directly by Li and Chen [25]. Their coordinated optimization model considered network topology, connecting pipe diameters, and flow allocation within a multi-source irrigation system, with construction and flow-distribution costs included in the objective. Although the present field uses a different supply configuration, their

findings support evaluating spatial arrangement and hydraulic loading together. In the proposed approach, hydraulic analysis is therefore essential for determining whether the selected pairing redistributes demand in a way that permits smaller commercial diameters.

The calculated maximum mainline velocity of 0.98 m s¹ suggests that alternative diameters could be investigated within the adopted velocity limit. However, satisfying that limit alone does not establish the least-cost solution. Optimized pipe diameters and lengths through a pipe length splitting method while maintaining hydraulic constraints, reporting a cost reduction of €21,930 in a network containing 107 hydrants [26] . Their results illustrate why diameter selection should be evaluated at the pipe-section level. For the present configuration, each candidate diameter must be checked across all operating shifts, particularly along routes with limited residual pressure.

Subplot 4b represented the governing hydraulic condition, with a displayed excess head of 0.0 m. Consequently, reducing diameters along its supply route could require additional pumping head even where flow velocity remains acceptable. Examined this relationship between critical hydrants, sectoring, and pumping arrangements in a drip irrigation network [27]. Their combined alternatives reduced annual energy consumption by up to 35.6%, while capital costs increased by approximately 15.9%. This comparison emphasizes the need to distinguish reductions in pipe procurement costs from improvements in total economic performance.

The verification results establish arithmetic consistency within the implemented model, but field measurements remain necessary to assess predictive accuracy. Incorporated pressure-dependent hydrant outflows into irrigation network optimization and evaluated trade-offs between installation costs and hydraulic performance [28]. Their application demonstrated the importance of realistic demand scenarios and outlet behaviour when identifying network deficiencies. In the present study, the small recalculation differences confirm consistency with the stated equations; they do not independently establish actual emitter discharge or irrigation uniformity.

Subplot 1a was absent from the hydraulic calculation, so the complete first paired shift has not yet been assessed. After correcting this connection and checking the distributor geometry, the proposed arrangement should be compared with adjacent-subplot grouping using identical irrigation requirements and hydraulic limits. Reporting section-specific diameters, installed lengths, procurement costs, and pumping requirements for both alternatives would establish whether the spatial pairing criterion provides a measurable design advantage.

Conclusion

This study developed a method for integrating the spatial pairing of irrigation subplots with hydraulic network analysis to support pipe diameter selection in drip irrigation systems. The method was applied to an irregular field of approximately 19.02 ha, in which 12 equal-area subplots were organized into six paired irrigation shifts, each with a planned discharge of approximately 111.24 m^3 h^{-1}. The max–min criterion provided a reproducible pairing arrangement with a minimum centroid separation of 287.20 m.

The hydraulic assessment demonstrated that equal total discharge does not result in equal network loading. Across the five complete paired shifts, the required pumping heads varied from 22.71 to 25.00 m, while mainline head losses ranged from 0.68 to 1.50 m. These differences highlight the importance of considering the locations of simultaneously operating subplots when sizing individual pipe sections. The maximum mainline velocity of 0.98 m s^{-1} satisfied the adopted

upper limit of 2.2 m s^{-1}. However, the negligible pressure margin at the governing subplot indicated that pipe diameter selection must also ensure adequate downstream pressure.

The calculation checks confirmed internal consistency within the precision of the reported values. Nevertheless, the hydraulic assessment remains preliminary because it covered 11 of the 12 planned subplots. Completing the missing connection, verifying the network geometry, and obtaining field measurements of pressure and discharge are necessary for final design verification. A comparison with adjacent-subplot grouping, incorporating commercial pipe diameters, installed lengths, procurement costs, and pumping requirements, is needed to quantify the potential economic benefits of the proposed method.

Overall, the proposed method provides a basis for incorporating irrigation-shift composition into the design and assessment of drip irrigation networks on irregular fields where pump capacity necessitates rotational irrigation.

Authors' contribution

Aybek Arifjanov: Supervision. Lukmon Samiev: Scientific consultation; Writing – review and editing. Sirojiddin Jalilov: Conceptualization; Literature review; Methodology; Software development; Hydraulic modelling; Formal analysis; Writing – original draft. Arken Tursun: Writing – review and editing. Khumora Jalilova: Visualization and figure preparation. Mardon Reimbayev: Data preparation and curation.

Ethics approval

Not applicable. This study did not involve human participants or animals.

Data Availability Statement

The data supporting the findings of this study are available from the corresponding author upon reasonable request. The study used field boundary geometry, subplot characteristics, irrigation shift configurations, pipe network parameters, and hydraulic calculation outputs. The main design parameters and calculated results are presented in the manuscript.

Conflict of interest

The authors declare that they have no known competing financial interests or personal relationships that could have influenced the work reported in this manuscript.

Table 1. List of abbreviations and their definitions

Abbreviation	Definition
EPANET	Software for hydraulic modelling of pressurized pipe networks
GA	Genetic Algorithm
GIS	Geographic Information System
GRASP	Greedy Randomized Adaptive Search Procedure
PSO	Particle Swarm Optimization
PSO–GA	Hybrid Particle Swarm Optimization–Genetic Algorithm
QGIS	Open-source Geographic Information System software

References

[1] Pourmahmoud, J.; Hashemy Shahdany, S.M.; Roozbahani, A. Practical Drought Risk Assessment and Management Framework: A Step toward Sustainable Modernization in Agricultural Water Management. *J. Hydrol. (Amst.)* **2024**, *644*. https://doi.org/10.1016/j.jhydrol.2024.132121.

[2] Elmahdi, A. Addressing Water Scarcity in Agricultural Irrigation: By Exploring Alternative Water Resources for Sustainable Irrigated Agriculture. *Irrigation and Drainage* **2024**, *73*, 1675–1683.

[3] Hou, P.; Ma, C.; Wang, J.; Li, Y.; Zhang, K.; Hou, S.; Li, J.; Sun, Z.; Xiao, Y.; Li, Y. Failure Behavior of Pressure Compensating Emitter under Different Operation Pressures in Drip Irrigation Systems. *Agric. Water Manag.* **2024**, *297*. https://doi.org/10.1016/j.agwat.2024.108835.

[4] Xing, S.; Du, K.; Liu, N.; Li, M.; Li, W.; Zhang, J.; Yin, F.; Zhang, J.; Wang, Z. Effect of Dynamic Pressure and Emitter Type on Irrigation and Fertigation Uniformity of Drip Irrigation Systems. *Agric. Water Manag.* **2025**, *312*. https://doi.org/10.1016/j.agwat.2025.109418.

[5] Wang, Y.; Zhang, Y.; Wang, W.; Liu, Z.; Yu, X.; Li, H.; Wang, W.; Hu, X. A Review of Optimal Design for Large-Scale Micro-Irrigation Pipe Network Systems. *Agronomy* **2023**, *13*.

[6] Fan, K.; Zhao, T.; Yu, X.; Wang, W.; Hu, X.; Ran, D.; Huo, X.; Wang, Y.; Pi, Y. Synchronization Optimization of Pipeline Layout and Pipe Diameter Selection in a Drip Irrigation Network System Based on the Jaya Algorithm. *Water* **2024**, *16*. https://doi.org/10.3390/w16202913.

[7] Peretti, F.; Menapace, A.; Zanfei, A.; Righetti, M. Optimal Irrigation Scheduling for Sustainable Agriculture: Minimising Energy Costs in Rotational Management. *Agric. Water Manag.* **2025**, *322*. https://doi.org/10.1016/j.agwat.2025.109986.

[8] Zhang, X.; Li, Y.; Wang, L.; Mao, B.; Yu, E.; Mu, Q.; Shan, M. Field-Calibrated Hydraulic Feedback for Optimizing Rotational Irrigation Grouping in Cotton Drip-Irrigation Networks. *Sci. Rep.* **2026**. https://doi.org/10.1038/s41598-026-67861-8.

[9] Lyu, H.; Guo, X.; Ai, Y.; Yang, A. Cooperative Optimization Design and Layout of Water Supply Facilities for Agricultural Sprinkler Irrigation Systems. *Appl. Sci.* **2026**, *16*. https://doi.org/10.3390/app16062741.

[10] Yang, F.; Li, H.; Jiang, Y. A Review of Pressure Regulation Technologies for Irrigation Pipeline Systems. *Agriculture* **2025**, *15*.

[11] González-Pavón, C.; Palau, C.V.; Juárez, J.M.; Guillem-Picó, S.; Balbastre-Peralta, I. Optimization of Multioutlet Hydrant Location and Pressurized Irrigation Network Layout Using the GRASP Metaheuristic. *J. Agric. Eng.* **2025**, *56*. https://doi.org/10.4081/jae.2025.1633.

[12] Li, M.; Bai, D.; Li, L. Optimization Design of Drip Irrigation System Pipe Network Based on PSO-GA: A Case Study of Northwest China. *Processes* **2025**, *13*. https://doi.org/10.3390/pr13051485.

[13] Carravetta, A.; Del Giudice, G.; Fecarotta, O.; Morani, M.C.; Ramos, H.M. A New Low-Cost Technology Based on Pump as Turbines for Energy Recovery in Peripheral Water Networks Branches. *Water* **2022**, *14*. https://doi.org/10.3390/w14101526.

[14] Paudel, P.P.; Adhikari, S. Technical Feasibility and Economic Analysis of Solar Photovoltaic Water Pumping System for Sustainable Irrigation in Nepal: A Case Study. *Int. J. Sustain. Eng.* **2025**, *18*. https://doi.org/10.1080/19397038.2025.2590115.

[15] Pedras, C.M.G.; Pereira, L.S.; Gonçalves, J.M. MIRRIG: A Decision Support System for Design and Evaluation of Microirrigation Systems. *Agric. Water Manag.* **2009**, *96*, 691–701. https://doi.org/10.1016/j.agwat.2008.10.006.

[16] Carrión, F.; Tarjuelo, J.M.; Hernández, D.; Moreno, M.A. Design of Microirrigation Subunit of Minimum Cost with Proper Operation. *Irrig. Sci.* **2013**, *31*, 1199–1211. https://doi.org/10.1007/s00271-013-0399-8.

[17] Moreno, M.A.; del Castillo, A.; Montero, J.; Tarjuelo, J.M.; Ballesteros, R. Optimisation of the Design of Pressurised Irrigation Systems for Irregular Shaped Plots. *Biosyst. Eng.* **2016**, *151*, 361–373. https://doi.org/10.1016/j.biosystemseng.2016.10.005.

[18] Baiamonte, G. Explicit Relationships for Optimal Designing Rectangular Microirrigation Units on Uniform Slopes: The IRRILAB Software Application. *Comput. Electron. Agric.* **2018**, *153*, 151–168. https://doi.org/10.1016/j.compag.2018.08.005.

[19] Palau, C.V.; Arviza, J.; Balbastre, I.; Manzano, J. DIMSUB, a Computer Program for Designing Microirrigation Subunits. Tool Definition and Case Studies. *Sci. Agric.* **2020**, *77*. https://doi.org/10.1590/1678-992x-2018-0184.

[20] Patel, N.; Rajput, T.B.S.; Kumar Dinkar, D.; Ram, S.; Singla, S.K. DOMIS: A Decision Support System for Design and Cost Estimation of Micro-Irrigation Systems. 2018, vol. 115.

[21] Sharu, E.H.; Ab Razak, M.S. Hydraulic Performance and Modelling of Pressurized Drip Irrigation System. *Water* **2020**, *12*. https://doi.org/10.3390/w12082295.

[22] Barberena, I.; Campo-Bescós, M.A.; Casalí, J. QDrip: A QGIS-Based Tool for the Spatial Layout and Cost Minimization of Drip Irrigation Subunits. In *Precision Agriculture '25*; publication details to be completed.

[23] Shaheemath Suhara, K.K.; Ravikumar, V.; Kannan, B.; Duraisamy, M.R.; Ganapati, P.S. Development of a Web-Based Simulation Application for Efficient Drip Irrigation Submain Design. *J. Appl. Nat. Sci.* **2023**, *15*, 1195–1203. https://doi.org/10.31018/jans.v15i3.4799.

[24] Córdoba, A.T.; Manzano, J.M. Reducing Flow Heterogeneity in Drip Irrigation Networks Using Genetic Algorithms. *Irrigation and Drainage* **2025**, *74*, 957–969. https://doi.org/10.1002/ird.3050.

[25] Li, Y.; Saiyue, C. Coordinated Optimization of Pipe Network Layout and Pipe Diameters in a Multi-Source Irrigation System. *Industrial Engineering Journal* **2024**, *27*. https://doi.org/10.3969/j.issn.1007-7375.220255.

[26] Samarinas, N.; Gravani, A.; Evangelides, C.; Loukas, A. A Smart Pipe Length Splitting Method for Cost Minimization of a Pressurized Irrigation Network: A Case Study in Greece. 2024.

[27] Khalil, E.M.; El-Fitiany, F.A.; Abourohiem, M.A.; Abdelrazek, A.M. Economic Assessment of Using Booster Pumps and Hydrant Sectoring in Pressurized Irrigation Networks (Case Study: Kostol Area, Egypt). *KSCE J. Civ. Eng.* **2024**, *28*, 495–501. https://doi.org/10.1007/s12205-023-0705-9.

[28] Creaco, E.; Barbero, G.; Montanaro, A.; Reduzzi, M. Effective Optimization of Irrigation Networks with Pressure-Driven Outflows at Randomly Selected Installation Nodes. *Sci. Rep.* **2023**, *13*. https://doi.org/10.1038/s41598-023-45844-3.

[29] Arifjanov, A.; Kaletova, T.; Abduraimova, D.; Samiev, L.; Jalilova, X. Evaluation of the Hydraulic Efficiency of the Sprinkler Irrigation System. In *IOP Conference Series: Earth and Environmental Science*; 2022, p. 12131.

[30] Arifjanov, A.; Samiev, L.; Abduraimova, D.; Jalilova, K. Sustainable Green Development: Water-Saving Irrigation Technologies. In *E3S Web of Conferences*; 2024, p. 5002.

[31] Aybek, A.; Luqmon, S.; Dilbar, A.; Khumora, J. Selecting an Effective Sprinkler Irrigation System Spacing: Based on Isodensity Contour Mapping, Voronoi-Like Connection, and Hotspot Clustering Models. *Water Conserv. Manag.* **2025**, *9*(3), 1–9. https://doi.org/10.26480/wcm.03.2025.446.454.

[32] Arifjanov, A.; Samiev, L.; Jalilova, K.; Jalilov, S.; Vokhidova, U.; Tursunova, E. Analysis and Design of the Trajectory of Water Droplets from Sprinklers Using Optical Observation and Mathematical Modeling. *J. Sustain. Dev. Energy Water Environ. Syst.* **2026**, *14*(1), 1–25. https://doi.org/10.13044/j.sdewes.d13.0647.

[33] Samiev, L.; Abduraimova, D.; Jalilova, K.; Gong, P.; Jalilov, S.; Liu, H.; Makhmudov, B.; Gafforova, M. Adapting China's Innovative Water-Saving Technologies to Uzbekistan: Needs, Opportunities, and Approaches. *Water Conserv. Manag.* **2026**, *10*(3), 667–677.